A bioactive triphasic ceramic-coated hydroxyapatite promotes proliferation and osteogenic differentiation of human bone marrow stromal cells

Manitha B. Nair,[1] Anne Bernhardt,[2] Anja Lode,[2] Christiane Heinemann,[2] Sebastian Thieme,[3] Thomas Hanke,[2] Harikrishna Varma,[1] Michael Gelinsky,[2] Annie John[1]

[1]*Biomedical Technology Wing, Sree Chitra Tirunal Institute for Medical Sciences and Technology, Poojapura P.O., Thiruvananthapuram, Kerala, India*

[2]*Institute of Materials Science, Max Bergmann Center of Biomaterials, Dresden University of Technology, Dresden, Germany*

[3]*Department of Pediatrics, University Clinic Carl Gustav Carus, Dresden University of Technology, Dresden, Germany*

Received 31 July 2007; revised 4 January 2008; accepted 4 April 2008
Published online 18 June 2008 in Wiley InterScience (www.interscience.wiley.com). DOI: 10.1002/jbm.a.32114

Abstract: Hydroxyapatite (HA) ceramics are widely used as bone graft substitutes because of their biocompatibility and osteoconductivity. However, to enhance the success of therapeutic application, many efforts are undertaken to improve the bioactivity of HA. We have developed a triphasic, silica-containing ceramic-coated hydroxyapatite (HASi) and evaluated its performance as a scaffold for cell-based tissue engineering applications. Human bone marrow stromal cells (hBMSCs) were seeded on both HASi and HA scaffolds and cultured with and without osteogenic supplements for a period of 4 weeks. Cellular responses were determined *in vitro* in terms of cell adhesion, viability, proliferation, and osteogenic differentiation, where both materials exhibited excellent cytocompatibility. Nevertheless, an enhanced rate of cell proliferation and higher levels of both alkaline phosphatase expression and activity were observed for cells cultured on HASi with osteogenic supplements. These findings indicate that the bioactivity of HA endowed with a silica-containing coating has definitely influenced the cellular activity, projecting HASi as a suitable candidate material for bone regenerative therapy. © 2008 Wiley Periodicals, Inc. J Biomed Mater Res 90A: 533–542, 2009

Key words: bioactive ceramics; mesenchymal stem cells; tissue engineering; cytocompatibility

INTRODUCTION

New strategies for engineering bone tissue are focused on defects with a critical size that will not heal spontaneously. These defects occur in millions of people affected by tissue loss from accidents, birth defects, or tumors.[1] Tissue engineering is a promising strategy for the repair of such defects. According to this concept, cells with osteogenic potential are isolated from the patient, expanded *in vitro*, and delivered to the defect within a three-dimensional construct designed to provide space for efficient delivery of the cells, control cell function and overall tissue shape. In short, this is based on the understanding of tissue formation and regeneration which aims to induce new functional tissue in contrast to classic biomaterial approaches using bare spare part implants.[2]

An ideal cell source for such applications should be easily expandable, nonimmunogenic, and should have a protein expression pattern similar to the tissue to be regenerated.[3] In this burgeoning field of bone tissue engineering, there has been special interest in multipotential cells located in the bone marrow known as bone marrow derived mesenchymal stem cells or bone marrow stromal cells (BMSCs). The idea that the bone marrow contains some kind of osteogenic precursor cells started in 1963, when Petrakova obtained osseous tissue by implanting pieces of bone marrow under the renal capsule.[4] Later, Caplan defined these cells as mesenchymal stem cells.[5] These cells are capable of self-renewal[6] and have the poten-

Correspondence to: A. John; e-mail: karippacheril@yahoo.com or ajkari@sctimst.ac.in

Contract grant sponsor: DST, India
Contract grant sponsor: DRDO
Contract grant sponsor: DAAD, Germany
Contract grant sponsor: CSIR

tial to differentiate toward various lineages including adipocytes, chondrocytes, osteoblasts, and other cell types of mesenchymal origin.[7,8]

The selection of the most appropriate material to produce a scaffold is another important step toward the construction of a tissue-engineered product, since it determines the success of the tissue–implant interaction. Among the different materials that have been proposed as bone substitutes, bioactive ceramics like hydroxyapatite (HA) have shown most promising results because of their osteoconductive properties, ability to integrate with the bone tissue, and absence of immune response.[9] But the main disability is the slow resorption rate of HA.[10] Concurrently, some studies have reported silica as an essential element for bone development and formation.[11] Silica-based bioactive glass plays an important role in the surface bioactivity by the exchange of ions at the glass tissue interface which results in the formation of carbonated HA layer, similar to the mineral phase of bone.[12] Here we propose an indigenous silica-based bioactive ceramic with dual advantages of both Si—O and HA, composed of a porous HA ceramic coated with calcium silicate, HA, and tricalcium phosphate (HASi). The material used in this study has thoroughly been characterized by FTIR spectroscopy, XRD, and EDAX which was described in detail elsewhere.[13] The bulk density of the material was 1.04 g cm^{-3} indicating 67% porosity of the material. Since the material is highly porous, the compressive strength is low in the range of 2–6 MPa.

Here, as part of the preclinical study, the behavior of human bone marrow stromal cells (hBMSCs) on HASi scaffolds was determined *in vitro* to ensure the suitability of this material for future clinical application. The functional role of HASi was envisaged by culturing hBMSC for 4 weeks and evaluated using microscopic, biochemical, and molecular biological techniques. For comparison, investigations with noncoated HA ceramics were performed simultaneously.

MATERIALS AND METHODS

Material preparation

HA powder was synthesized by a wet precipitation method involving calcium nitrate and ammonium dihydrogen phosphate in the stoichiometric proportion at a pH of 11 and a temperature of 80°C. The precipitated HA powder was freeze-dried and washed with distilled water to get rid of surface impurities such as nitrate and ammonium ions. HA powder having particle size less than 125 μm was mixed with aqueous solution of poly (vinyl alcohol) and glutaraldehyde solution and stirred for 30 min. To the resulting frothy slurry, benzoyl peroxide dispersed in benzene and *N*,*N*′-dimethylaniline were added and stirred for thorough mixing. The resulting frothy and viscous slurry was poured into plastic molds and allowed to dry at room temperature. After drying, the blocks were biscuit-fired at 300°C for 1 h to remove the binder and then sintered at temperature between 1100 and 1300°C for 1 h to get porous ceramics. The HA blocks prepared by the aforementioned process were dipped in a silica sol prepared by the hydrolysis of tetraethyl orthosilicate in ethanol–water system for 1 min. The resultant coated HA ceramic was sintered at 1200°C for 2 h to get a coating over HA. The samples were later polished to get a size of 5 mm diameter and 5 mm thickness and subjected to ultrasonic cleaning for the complete removal of fine powders adhered over the surface. HA without the coating, but synthesized under the same conditions, was used as control for all of the experiments. Both HA and HASi are porous in nature with pore size ranging between 50 and 500 μm (Fig. 1). Prior to cell seeding, the materials were steam-sterilized and conditioned by placing in Dulbecco's modified eagle's medium (DMEM) and incubated at 37°C for 24 h.

Cell culture

hBMSC were isolated from bone marrow aspirates of a healthy human donor (age 31; kindly provided by Sabine Boxberger, University Hospital Carl Gustav Carus Dresden). Expansion of the cells was performed in DMEM with low glucose (Biochrom, Berlin, Germany), containing 10% fetal calf serum (FCS; Biochrom), 10 U/mL penicillin, and 100 μg/mL streptomycin (Biochrom) at 37°C in a humidified, 7% CO_2/93% air incubator. Cells of passage 3–5 were used for all the experiments. After trypsinization, cells were harvested and seeded (1×10^5 cells per scaffold) on all sides of both HA and HASi, placed in 48-well standard tissue culture plates under static condition (Nunc, Wiesbaden, Germany). The experiments were divided into two sets. In one set, the cell-seeded constructs were cultivated in DMEM containing 2% FCS, 10 U/mL penicillin, and 100 μg/mL streptomycin. After 1 day of cultivation, cells were induced for osteogenic differentiation (OS+) by the addition of $10^{-7}M$ dexamethasone (Sigma-Aldrich, Taufkirchen, Germany), 3.5 m*M* β-glycerophosphate (Sigma), and 50 μ*M* L-ascorbic acid-2-phosphate (Sigma) to the medium. In a second set, the cell-seeded constructs were cultivated in DMEM containing 2% FCS, 10 U/mL penicillin, and 100 μg/mL streptomycin without osteogenic differentiation (OS−). The medium change was done twice weekly.

Confocal laser scanning microscopy

Confocal laser scanning microscopy (cLSM) studies were performed using a cLSM 510 Meta (Zeiss, Jena, Germany) mounted on an upright Axioscope 2 FS mot and equipped with an additional argon ion (Ar^+) laser, helium–neon (HeNe) laser and NIR-femtosecond titanium-sapphire laser for 2-photon excitation (Coherent Mira 900F).

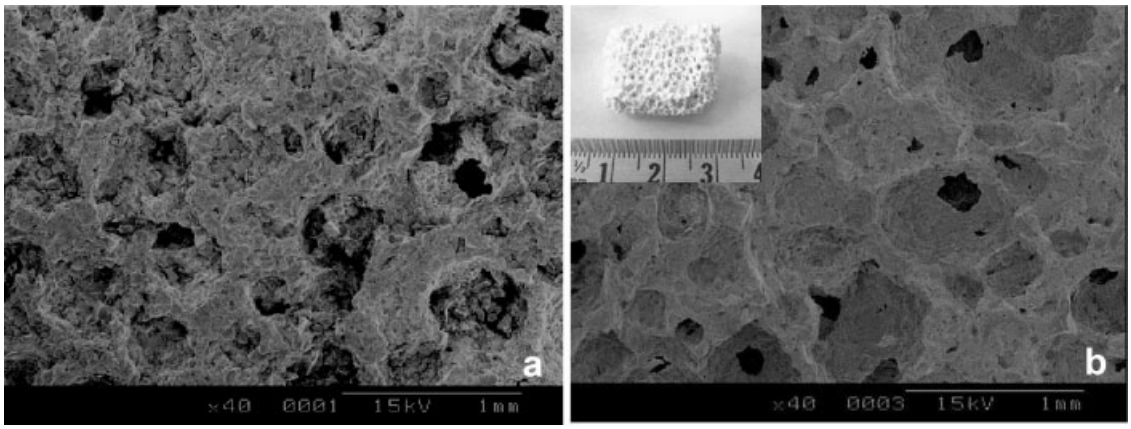

Figure 1. SEM showing the interconnected porous nature of (a) HA and (b) HASi. The inset shows the gross image of HASi.

Cell viability

The viability of hBMSC on both HA and HASi was determined using LIVE/DEAD® viability/cytotoxicity kit (Molecular Probes, Eugene). After 24 h of cell seeding, the samples were incubated with DMEM containing 4 m*M* calcein AM and 2 m*M* ethidium homodimer-1 for 30 min. The nonfluorescent calcein AM permeates the intact membrane of living cells and is converted into fluorescent calcein. The ethidium homodimer-1 enters damaged cells and is fluorescent when bound to nucleic acids. The cell-seeded scaffolds were washed with phosphate buffered saline (PBS) thrice and imaged. Calcein fluorescence was excited with the Ar^+ laser at 495 nm, and ethidium homodimer-1 excitation was carried out using 528-nm HeNe laser.

ALP staining

The cell-seeded HA and HASi samples cultured with (OS+) and without (OS−) osteogenic supplements for 10 days were washed with PBS and fixed with 3.7% formaldehyde. After permeabilizing with 0.2% Triton-X-100 in PBS, samples were blocked with 3% bovine serum albumin in PBS for 30 min. Staining was performed with TRITC-phalloidin (Sigma) for cytoskeletal actin and ELF-97 (Molecular probes) for ALP activity. Excitation of ELF-97 was carried out with the NIR-fs-laser at 770 nm (emission 537–569 nm), and TRITC-phalloidin was excited with the HeNe laser at 528 nm.

Scanning electron microscopy

For examination of the microstructure, both HA and HASi blocks were mounted on stubs, gold coated using an ion sputter (Hitachi E101) and analyzed by scanning electron microscopy (SEM; Hitachi S2400). Attachment and spreading of the hBMSC after 1 and 24 h as well as the morphology of osteogenic-induced (OS+) hBMSC on HA and HASi were assessed after 14 and 28 days of culture by SEM. The cell-seeded samples were fixed with 2% glutaraldehyde in PBS. Dehydration was performed with slow water replacement by a series of graded ethanol solutions with final dehydration in absolute ethanol before critical-point drying using a CPD030 apparatus (BAL-TEC, Liechtenstein). The materials were mounted on stubs, gold-coated using a Sputter Coater SCD 050 (BAL-TEC) and analyzed by SEM (IDSM 982 Gemini, Zeiss, Jena, Germany and Philips XL 30/ESEM operating in SEM mode).

Biochemical assays

Biochemical assays of osteogenic-induced (OS+) and non-induced (OS−) cells on HA and HASi were performed at days 1, 4, 11, 14, 21, and 28 of cultivation. To this end, cell-seeded samples ($n = 3$) were washed twice with PBS and kept at −80°C until analysis. For cell lysis, these frozen samples were thawed for 20 min on ice and thereafter incubated with 1% Triton-X 100 in PBS for 50 min combined with a sonication step for 10 min. Aliquots of each lysate were used for determining cell viability [lactate dehydrogenase (LDH) activity], proliferation (DNA content), and osteogenic differentiation (OD) (ALP activity).

LDH activity

The viability of osteogenic-induced (OS+) cells after 4, 11, and 21 days of cultivation was determined by measurement of cytosolic LDH activity using Cytotox96 kit (Promega, Madison). An aliquot of each cell lysate (50 μL) was mixed with LDH substrate (50 μL) at room temperature, and the enzymatic reaction was stopped after 30 min with 0.1*M* acetic acid. The absorbance was read at 492 nm with a multifunction micro plate reader (Spectra fluor plus, Tecan, Crailsheim, Germany). A calibration line was plotted with an increase in the concentration of cells.

DNA content

The adhesion of hBMSC after 30 min, 1, 4, and 24 h and proliferation of osteogenic-induced (OS+) and noninduced (OS−) cells after 1, 4, 7, 11, 14, 21, and 28 days of cultivation was determined using Picogreen® dsDNA Quantitation rea-

TABLE I
Primers and Probes for Real-Time PCR

Gene	Accession Number	Forward and Reverse Primer (5′-3′)	TaqMan Probe (5′-3′)[a]
gapdH	AF261085[b]	GAAGGTGAAGGTCGGAGTCGAAGAT GGTGATGGGATTTC	CAAGCTTCCCGTTCTCAGCC
alpL	ENST00000344573[c]	CCGTGGCAACTCTATCTTTGGCAGGC CCATTGCCATACAG	CCATGCTGAGTGACACAGACAAGAAGCC
bspII	ENST00000226284[c]	AAGCATGCCTACTTTTATCCTCATTCA TTCGATTCTTCATTGTTTTCTCC	TTTCCAGTTCAGGGCAGTAGTGACTCATCC

[a]Probes were labeled with FAM (6-carboxyfluorescin) at the 5′end and TAMRA (*N*,*N*,*N*′,*N*′-teratmethyl-6-carboxyrhodamine) at the 3′end.
[b]Entrez accession number.
[c]Ensembl accession number.

gent (Molecular probes) according to manufacturers instructions. The intensity of fluorescence was measured with a multifunction microplate reader (Spectra fluor plus, Tecan) at an excitation and emission wavelength of 485/535 nm. Relative fluorescence units were correlated with cell number using a calibration line constructed from cell suspensions with increasing concentrations of cell numbers.

ALP activity

To study differentiation of hBMSC induced in osteogenic lineage (OS+), ALP activity was measured after 1, 4, 7, 11, 14, 21, and 28 days of cultivation. Noninduced (OS−) hBMSC were taken as the control. The ALP activity measured for each lysate was related to the cell number determined by the Picogreen DNA assay to calculate the specific ALP activity for each sample. Biochemical quantification of ALP activity was based on the hydrolysis of *p*-nitrophenyl phosphate (Sigma) to *p*-nitrophenol. An aliquot of each cell lysate (25 μL) was added to ALP reaction buffer (125 μL), containing 1 mg/mL *p*-nitrophenyl phosphate (Sigma), 0.1*M* diethanolamine, 1% Triton X-100 and 1 mM $MgCl_2$ (pH 9.8), and the mixture was incubated at 37°C for 30 min. 1 M NaOH was added to stop the enzymatic reaction. After centrifugation at 16,000 *g* for 10 min, 170 μL of each supernatant was transferred to a microtiter plate and the absorbance was read at 405 nm with a multifunction microplate reader (Spectra fluor plus, Tecan). A calibration line was constructed from different concentrations of *p*-nitrophenol.

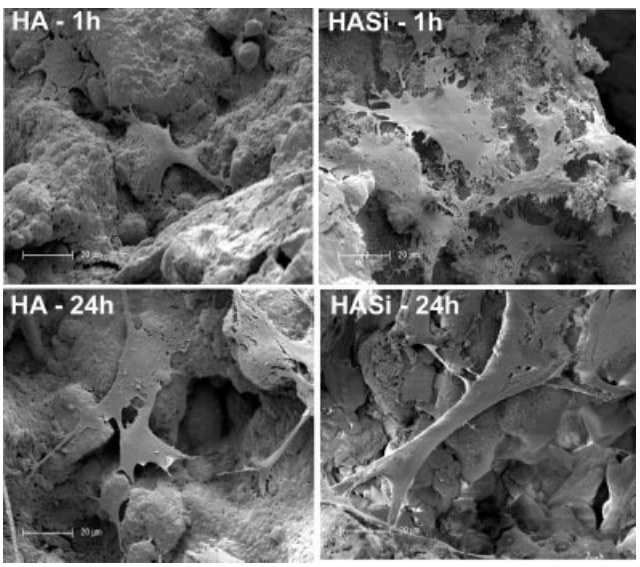

Figure 2. SEM showing the adhesion of hBMSC on HA and HASi. At 1 h, cells started spreading and at 24 h cells got enlarged and adhered very firmly on both HA and HASi. When compared, HASi was found to provide a more favorable platform.

Real-time PCR

The gene expression of ALP and bone sialoprotein II (BSP II) in osteogenic-induced (OS+) and noninduced (OS−) cells grown on HA and HASi was evaluated by real-time PCR using TaqMan probes which were labeled with FAM (6-carboxyfluorescein) at the 5′-end and TAMRA (*N*,*N*,*N*′,*N*′-tetramethyl-6-carboxyrhodamine) at the 3′-end. At predetermined time points (days 1, 4, 11, and 14) after culture, the cell-seeded scaffolds were washed twice with PBS, and the total RNA was isolated using the RNeasy Mini Kit (Qiagen, Hilden, Germany) following the procedure described by the manufacturer. cDNA was transcribed using 200 U of Superscript II

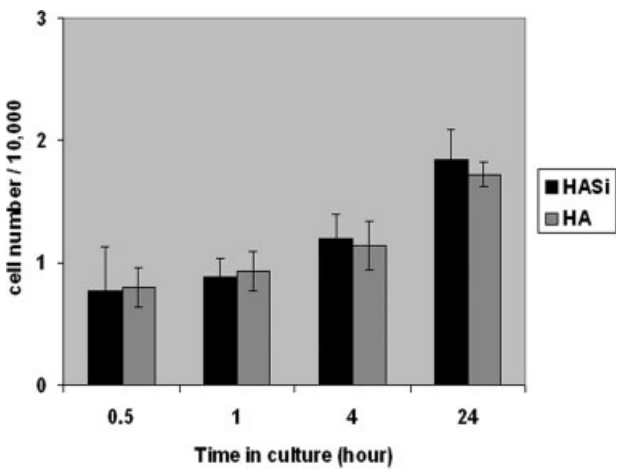

Figure 3. hBMSC adhered on HA and HASi within an initial time period of 24 h, determined by the Picogreen DNA assay after cell lysis. $n = 6$ (mean ± standard deviation). There was no significant difference between HA and HASi.

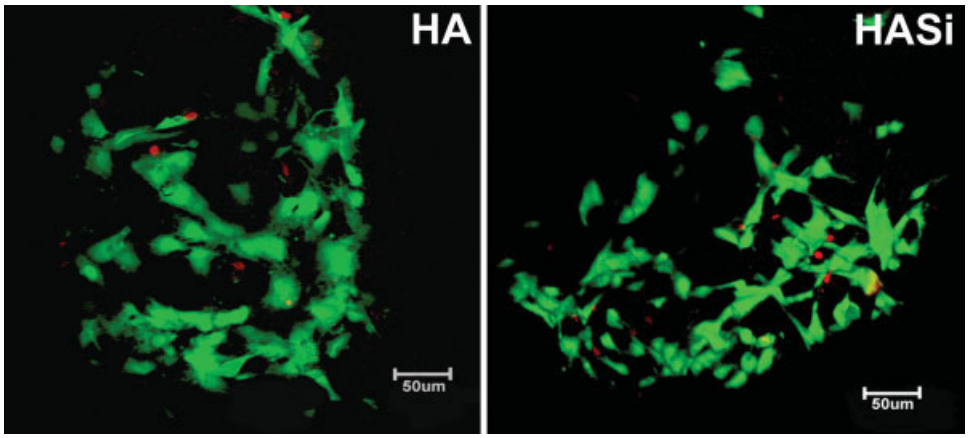

Figure 4. cLSM showing viability of hBMSC on HA and HASi 24 h after seeding. Living cells converted calcein AM to fluorescent calcein (green) and DNA of death cells was stained by ethidium homodimer-1 (red). [Color figure can be viewed in the online issue, which is available at www.interscience.wiley.com.]

Reverse Transcriptase (Invitrogen, Carlsbad, CA), 0.5 m*M* dNTPs (Invitrogen), and 12.5 ng/μL random hexamers (MWG Biotech, Ebersberg, Germany) and 40 U of RNase inhibitor RNase OUT (Invitrogen). TaqMan PCRs were carried out in an ABI PRISM 7700 (Applied Biosystems, Foster City, CA). The accumulation of PCR products was quantified using the comparative CT method in which the accumulated PCR products of each of the genes examined is normalized to the housekeeping gene GAPDH in the corresponding samples. The primers (MWG Biotech) for each gene are summarized in Table I.

Statistics

Three samples were used for each parameter in all quantitative experiments. From this, all measurements were done in duplicate. Each parameter is expressed as mean of all values ± standard deviation. Single factor analysis of variance was employed to assess the statistical significance of results. *p*-values less than 0.01 were considered significant for all analyses.

RESULTS

Cell adhesion

Initial adhesion of hBMSC on HA and HASi was evaluated qualitatively using SEM and quantitatively by the Picogreen DNA assay. After 1 h of cell seeding, SEM images depicted round morphology for the cells on both substrates, with few spread cells on HASi. The adhesion and spreading became more obvious 4 h after seeding and after 24 h, cells appeared well spread to both HASi and HA (Fig. 2). These findings were supported by the simultaneous quantitative determination of the number of attached cells (Fig. 3). There was no significant difference between the cells that adhered on HA and HASi at an early period of 24 h.

Cell viability

The presence of viable cells on both HA and HASi was visualized using cLSM after 24 h of seeding, which depicted a high ratio of living cells on both substrates (Fig. 4). Quantitative LDH activity measurement revealed a significant higher rate of viability on HASi compared to HA ($p < 0.001$) on day 21 (Fig. 5).

Cell proliferation

The cell number on HA and HASi determined from the analysis of DNA content after cell lysis was observed to increase over the whole cultivation period of 28 days. At later time points of cultivation

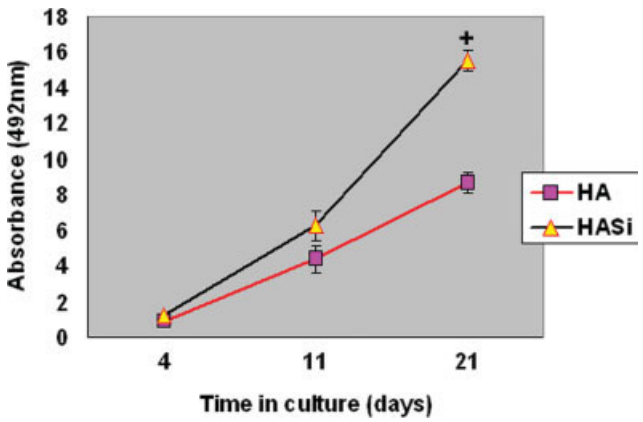

Figure 5. Viability of osteogenic-induced hBMSC on HA and HASi determined by measurement of LDH activity after cell lysis. $n = 6$ (mean ± standard deviation). On day 21, LDH activity was significantly ($p < 0.001$) higher (+) on HASi. [Color figure can be viewed in the online issue, which is available at www.interscience.wiley.com.]

(day 14, 21, and 28), the number of osteogenic-induced hBMSC on HASi was significantly higher than that on HA ($p < 0.001$) [Fig. 6(a)]. Osteogenic-induced hBMSC also showed significant higher proliferation rates compared to noninduced hBMSC on both HA [Fig. 6(b)] and HASi [Fig. 6(c)] from days 14 to 28 ($p < 0.001$), which was supported by SEM analysis on HASi (Fig. 7). On day 14, cells covered the material homogenously forming a sheet-like canopy [Fig. 7(a)]. On day 28, cultures developed a continuously interconnected network of extracellular matrix over the material, but without pore occlusion or pore bridging [Fig. 7(b)].

Osteogenic differentiation

Specific ALP activity

An increase of specific ALP activity at early time points of cultivation was detected for osteogenic-induced (OS+) hBMSC on HA and HASi, indicating differentiation toward the osteoblastic lineage. Specific ALP activity of OS+ cells on days 11, 14, and 21 was significant higher on HASi compared to HA ($p < 0.01$). ALP activity of noninduced (OS−) hBMSC remained unchanged over the whole culture period of 28 days (Fig. 8). ALP activity of osteogenic-induced hBMSC on HA and HASi was furthermore demonstrated by ELF-97 staining followed by cLSM investigation (Fig. 9).

Gene expression

Differentiation of osteogenic-induced (OS+) hBMSC on HA and HASi was further demonstrated by an increase in the relative expression of the osteogenic markers ALP and BSPII. In the absence of dexamethasone, β-glycerophosphate, and L-ascorbic acid, no increase of expression was detected for both osteogenic markers (Figs. 10 and 11). The relative ALP expression on HASi was higher compared to HA. However, the maximum ALP expression was detected earlier on HA (Fig. 10). A slightly higher maximal expression of BSP II was detected on HASi (found on day 14) compared to HA (found on day 11) (Fig. 11).

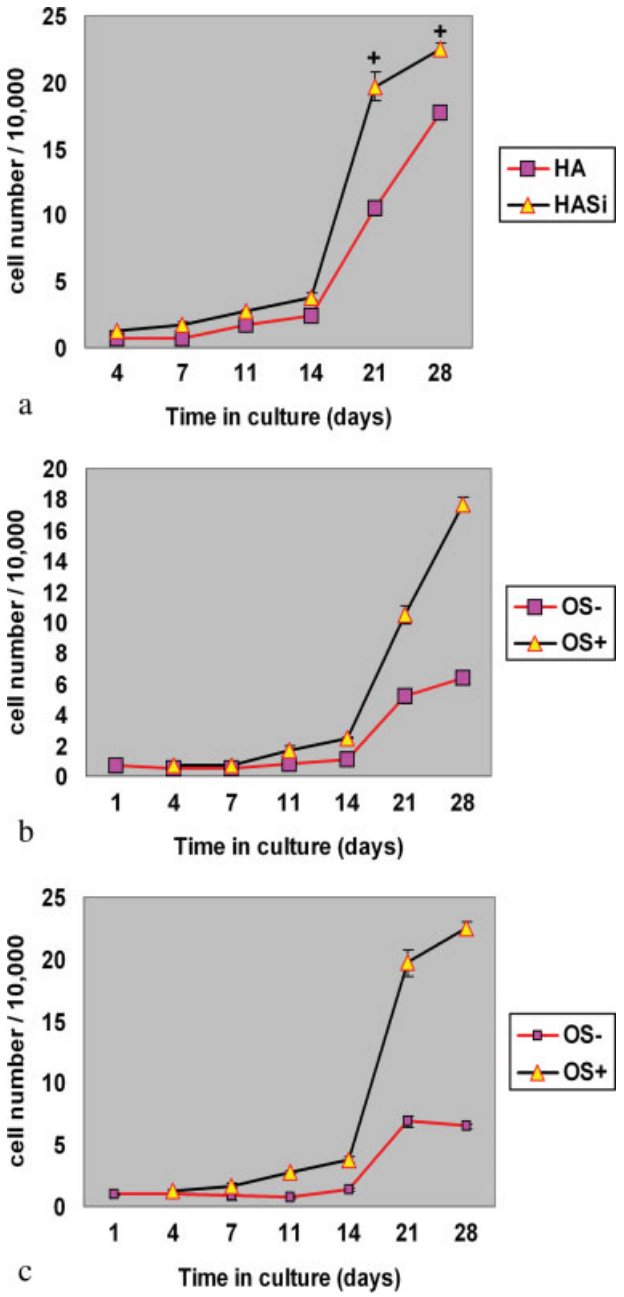

Figure 6. Proliferation of cells on HA and HASi, determined by measurement of the DNA content at different time points (Picogreen DNA assay) $n = 6$ (mean ± standard deviation). Cell number was calculated from DNA content using a calibration line of known cell numbers. (a) The proliferation of osteogenic-induced cells on HASi compared to HA. Cell number on HASi was significantly higher (+) compared to HA on days 21 and 28 ($p < 0.001$). (b) Proliferation of osteogenic induced (OS+) versus non-induced cells (OS−) on HA. (c) Proliferation of osteogenic induced (OS+) versus noninduced (OS−) cells on HASi. [Color figure can be viewed in the online issue, which is available at www.interscience.wiley.com.]

DISCUSSION

Tissue engineering generally requires the use of scaffolds that serve as three-dimensional templates for initial cell attachment, proliferation, and subsequent tissue formation. Hence, the capability of a triphasic ceramic-coated HA to provide a good microenvironment for adequate adherence, multiplication, and differentiation of hBMSCs was evaluated in this study. The material has thoroughly been character-

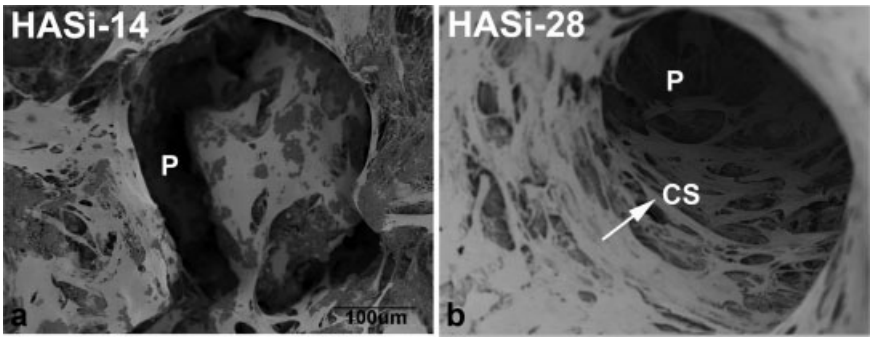

Figure 7. SEM images of osteogenic-induced hBMSC after cultivation for (a) 14 and (b) 28 days on HASi. Cells covered the material homogenously showing a cell-sheet like appearance without pore occlusion and pore bridging. p: pore and CS: cell sheet.

ized by FTIR spectroscopy, XRD, and EDAX, which was described in detail elsewhere.[13]

The confocal micrographs portrayed similar viability of hBMSC on both HASi and HA. Furthermore, cell viability was determined quantitatively by measurement of LDH activity. The conventional cytotoxicity detection protocols based on LDH activity assays rely upon the quantification of the enzyme activity released into the cell culture medium due to the damage of the cell membrane. In contrast, we have quantified the amount of LDH activity in undamaged cells after lysis as described by Sepp et al.[14] Thus, LDH activity is related to the viability of cells. LDH activity values were higher on HASi samples suggesting that more viable cells were present on this material compared to HA. This is in accordance to a study of Valerio et al.,[15] who have also reported the increased viability of rat osteoblasts cultured in the presence of bioactive glass compared to that of biphasic calcium phosphate ceramic and standard tissue culture plate.

Adhesion of hBMSC on HA and HASi ceramics was quantified by the Picogreen DNA assay within an initial time period of 24 h. The number of cells adhered on both HA and HASi was almost similar at different time points within 24 h. On the other hand, our qualitative adhesion study hints at an earlier spreading of hBMSC on HASi compared to HA. On conclusion, both HASi and HA surfaces are well suited for cell attachment, with only minor preference of the silica-coated surface. The enhanced initial adhesion and spreading of cells may be partly dependent on proteins adsorbed onto the surface of HASi. The surface chemistry of silica-based materials are amenable to very strong and often irreversible adsorption of proteins which is attributed to high negative surface charge density generated by surface silinols (Si—OH).[16] These will bind to various functional groups of a protein via hydrogen bonding and long-range electrostatic ionic amine bonds ($Si—O^-$ $^+H_3N—$).[17] Similarly, in a comparative study with calcium silicate and tricalcium phosphate ceramics, enhanced cell spreading and growth was found on calcium silicate substitutes compared to tricalcium phosphate ceramics.[18]

With respect to hBMSC cultured with osteogenic supplements, a higher proliferation rate was found on HASi compared to that measured on HA. *In vitro* studies by Botelho et al.[19] proved that human osteoblasts are affected by the presence of silicon in the HA substrate. Another study has also reported the improved cell adhesion and proliferation on a hybrid hydrogel based on 2-hydroxyethylmethacrylate and fumed silica nanoparticles than on pure poly(hydroxyethyl methacrylate).[20] Contemporarily, several studies have also indicated poor proliferation rates of osteoblasts on sintered HA.[21,22] Nonetheless, porous HA in our study proved to promote proliferation of osteogenic-induced hBMSC even without the silica coating. The effect of HA on cell proliferation may depend on its physical and chemical characteristics like crystallinity, particle size, and surface topography, and therefore different cell behavior can be expected for diverse HA-based scaffolds. While

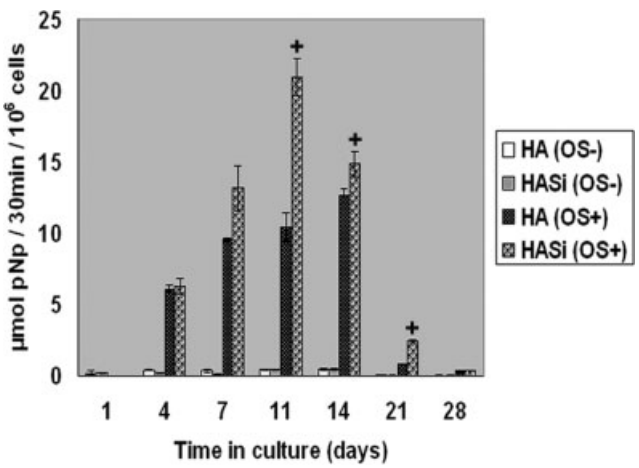

Figure 8. Specific ALP activity of osteogenic induced and noninduced hBMSC on HA and HASi. $n = 6$ (mean ± standard deviation). HASi performed significantly (+) on days 11, 14, and 21 as compared to HA ($p < 0.01$).

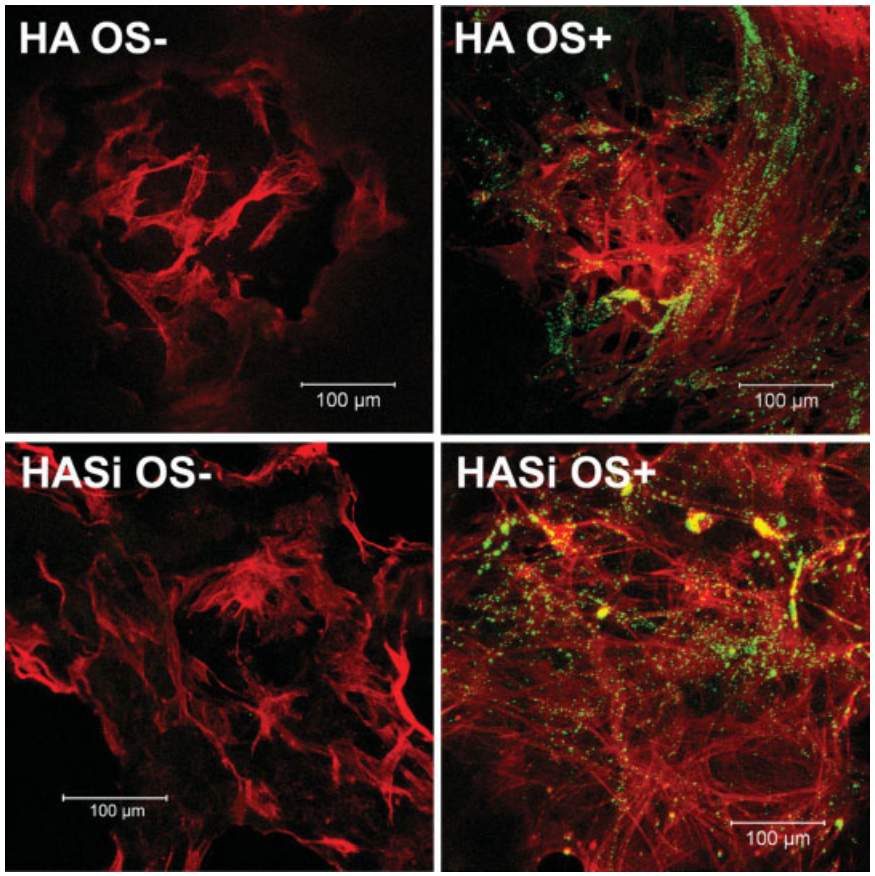

Figure 9. cLSM showing ALP activity of osteogenic induced hBMSC on HA and HASi after 10 days of cultivation. Staining was performed with ELF-97 for ALP activity (yellowish green) and TRITC-phalloidin for cytoskeletal actin (red). hBMSC without osteogenic induction was taken as negative control (day 10). [Color figure can be viewed in the online issue, which is available at www.interscience.wiley.com.]

comparing the proliferation of hBMSC cultured with and without osteogenic supplements, higher rates were observed for the osteogenic-induced (OS+) hBMSC on both HA and HASi. Some studies have

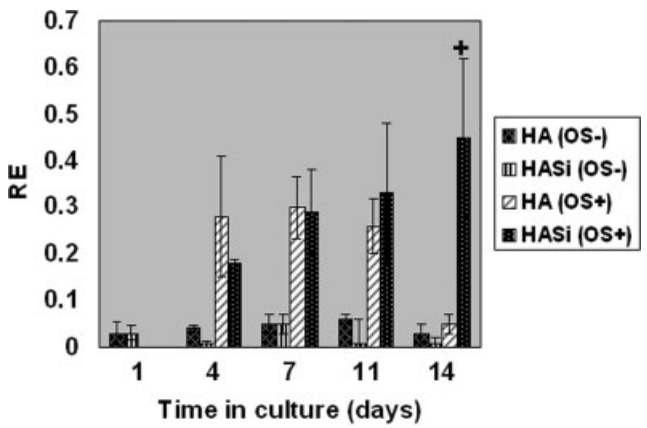

Figure 10. ALP expression of osteogenic-induced and non-induced hBMSC on HA and HASi determined by real-time PCR, $n = 6$ (mean ± standard deviation). RE = ratio of gene expression relation to expression of GAPDH, a house keeping gene. ALP expression on HASi (OS+) was significantly higher (+) compared to HA (OS+) on day 14 ($p < 0.01$).

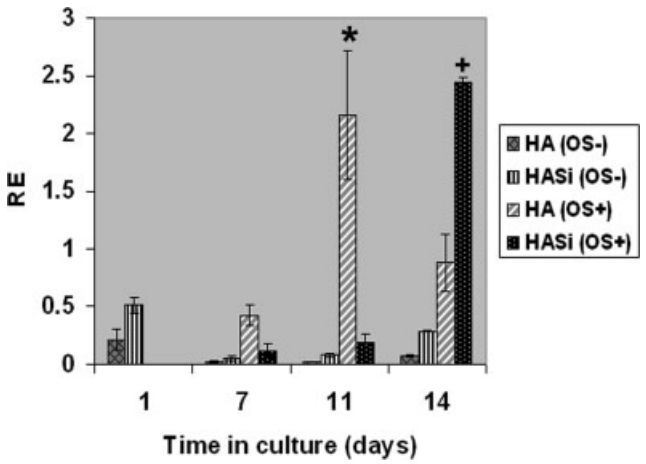

Figure 11. BSP II expression of osteogenic induced and noninduced hBMSC on HA and HASi, determined by real-time PCR, $n = 6$ (mean ± standard deviation). RE = ratio of gene expression relation to expression of GAPDH, a house keeping gene. On day 11, BSP II expression on HA (OS+) was significantly higher (*) compared to HASi (OS+) ($p < 0.001$). On day 14, expression of BSP II was significantly higher (+) on HASi (OS+) than on HA (OS+) ($p < 0.01$).

demonstrated a proliferation stimulating effect of osteogenic supplements on cells cultivated on standard tissue culture plates.[23,24]

Alkaline phosphatase is an enzyme that is normally present in high concentration in growing bone, essential for the deposition of minerals and is considered as an early bone marker. Accordingly, the specific ALP activity (ALP activity per cell) of osteogenic-induced (OS+) hBMSC on both HA and HASi significantly increased up to 14 days in culture followed by a decline in activity. Evidence exists that HA promotes osteogenic cell differentiation.[25] When HASi was compared with HA, cells on HASi showed a significantly stronger increase in specific ALP activity during cultivation time. The positive impact of bioactive glass surfaces on osteogenic differentiation has been reported in previous studies.[26,27] One explanation for the influence of bioactive glass on osteogenic differentiation is the Si content which may affect bone cell activity. Rhee et al.[28] showed a better biological performance like attachment, proliferation, and differentiation of primary cultured mouse calvarial osteoblast cells on PMMA/silica hybrid material when compared to PMMA alone. Bone nodules form much earlier on silica surfaces than control which can be explained by the uptake of silicic acid by osteoblasts, inducing early mineralization.[29] Our findings concerning specific ALP activity of osteogenic-induced (OS+) cells on HA and HASi scaffolds were supported by the analysis of ALP expression by real-time PCR. Thus, the highest ALP expression was found on HASi. A number of studies suggest a promoting effect of ionic dissolution products of bioactive glass (mainly Si^{4+} and Ca^{2+}) on ALP expression of osteogenic cells and osteoblast-like cells.[30–32] Coincident to ALP, the expression of BSP II was also increased upon osteogenic induction on both materials with a slightly higher value on HASi.

Generally, cell proliferation and differentiation are two interdependent processes having a counteracting relationship. When the cells go through differentiation lineage with subsequent induction of genes associated with matrix maturation and mineralization, a decline in cell proliferation is reported on conventional tissue culture plate.[33] However, in our study, HASi was capable of inducing osteogenesis and cell proliferation in a parallel relationship. Recently, results with human MSCs and primary human fibroblasts indicated that growth on a denatured collagen (DC) matrix results in the reduction of the rate of cellular aging with simultaneous increase in the retention of osteogenic-specific functions and markers upon treatment with osteogenic stimulants.[34,35] Another study demonstrated a significant *ex vivo* expansion as well as expression of adipogenic markers of late passage MSC cultured on the DC matrix similar to early passage cells and in contrast to late passage MSCs cultured on standard tissue culture plate.[36] In addition, results of cell culture studies with rat calvarial osteoblasts showed both an enhanced proliferation and differentiation on a *O*-phospho-L-serine modified calcium phosphate bone cement.[37] Thus the ultimate fortune of cells is determined by the respective matrix/substratum, but the actual molecular mechanism is still a question. Nevertheless, the ability of HASi in maintaining cell expansion and differentiation is a promising approach to address the problem of bone regeneration in older patients where more extensive *in vitro* expansion of smaller number of stem/progenitor cells is needed.

CONCLUSION

In summary, the bioactivity of HASi was investigated in comparison with noncoated HA in an *in vitro* culture system. Our data demonstrated that HA coated with a calcium silicate containing layer encouraged cell proliferation and osteogenic differentiation of human bone marrow-derived stromal cells. This newly developed indigenous material with respect to its structural and functional properties is proposed as a favorable bone substitute for the healing of bone defects which still remains a challenging problem to orthopedic surgery.

The authors thank The Director of SCTIMST for support and Suresh Babu for material preparation. They acknowledge Sabine Boxberger, Medical Clinic I, University Hospital Dresden, for kindly providing hBMSC.

References

1. Maurilio M, Elizaveta K, Vladimir M, Andrei L, Sergej K, Rodolfo Q, Maddalena M, Ranieri C. Stem cells associated with macroporous bioceramics for long bone repair: 6- to 7-year outcome of a pilot clinical study. Tissue Eng 2007;13:947–955.
2. Salgado AJ, Coutinho OP, Reis RL. Bone tissue engineering: State of the art and future trends. Macromol Biosci 2004;4:743–765.
3. Zangi L, Rivkin R, Kassis I, Levdansky L, Marx G, Gorodetsky R. High-yield isolation, expansion and differentiation of rat bone marrow-derived mesenchymal stem cells with fibrin microbeads. Tissue Eng 2006;12:2343–2354.
4. Petrakova KV. Heterotopic ossification in the rat kidney in ischemia. Arkh Anat Gistol Embriol 1963;44:112–116.
5. Caplan AI. Mesenchymal stem cells. J Orthop Res 1991;9:641–650.
6. Caplan AI. Mesenchymal stem cells: Cell based reconstructive therapy in orthopaedics. Tissue Eng 2005;11:1198–1211.
7. Haynesworth SE, Goshima J, Goldberg VM, Caplan AI. Characterization of cells with osteogenic potential from human marrow. Bone 1992;13:81.

8. Pittenger MF, Mackay AM, Beck SC, Jaiswal RK, Douglas R, Mosca JD, Moorman MA, Simonetti DW, Craig S, Marshak DR. Multilineage potential of adult human mesenchymal stem cells. Science 1999;284:143–147.
9. Neo M, Kotani S, Nakamura T, Yamamuro T, Ohtsuki C, Kokubo T, Bando Y. A comparative study of ultra structure of the interfaces between four kinds of surface-active ceramic and bone. J Biomed Mater Res 1992;26:1419–1432.
10. Vuola J, Taurio R, Goransson H, Asko-Seljavaara S. Compressive strength of calcium carbonate and hydroxyapatite implants after bone-marrow-induced osteogenesis. Biomaterials 1998;19:223.
11. Carlisle EM. Silicon: A possible factor in bone calcification. Science 1970;167:279–280.
12. Ning CQ, Greish Y, EL-Ghannam A. Crystallization behaviour of silica-calcium phosphate biocomposites: XRD and FTIR studies. J Mater Sci Mater Med 2004;15:1227–1235.
13. Nair MB, Babu S, Varma HK, John A. A triphasic ceramic coated porous hydroxyapatite for tissue engineering application. Acta Biomater 2008;4:173–181.
14. Sepp A, Binns RM, Lechler RI. Improved protocol for colorimetric detection of complement-mediated cytotoxicity based on the measurement of cytoplasmic lactate dehydrogenase activity. J Immunol Methods 1996;196:175–180.
15. Valerio P, Guimaraes MH, Pereira MM, Leite MF, Goes AM. Primary osteoblast cell response to sol-gel derived bioactive glass foams. J Mater Sci Mater Med 2005;16:851–856.
16. Lobel KD, Hench LL. In vitro adsorption and activity of enzymes on reaction layers of bioactive glass substrates. J Biomed Mater Res 1998;39:575–579.
17. Messing RA. Molecular inclusions. Adsorption of macro molecules on porous glass membranes. J Am Chem Soc 1969;91: 2370–2371.
18. Ni S, Chang J, Chou L, Zhai W. Comparison of osteoblast-like cell responses to calcium silicate and tricalcium phosphate ceramics in vitro. J Biomed Mater Res B Appl Biomater 2007;80:174–183.
19. Botelho CM, Brooks RA, Best SM, Lopes MA, Santos JB, Rushton N, Bonfield W. Human osteoblast response to silicon-substituted hydroxyapatite. J Biomed Mater Res 2006;79: 723–730.
20. Schiraldi C, D'Agostino A, Oliva A, Flamma F, De Rosa A, Apicella A, Aversa R, De Rosa M. Development of hybrid materials based on hydroxyethylmethacrylate as supports for improving cell adhesion and proliferation. Biomaterials 2004; 25:3645–3653.
21. Puleo DA, Holleran LA, Doremus RH, Bizios R. Osteoblast responses to orthopedic implant materials in vitro. J Biomed Mater Res 1991;25:711–723.
22. Massas R, Pitaru S, Weinreb MM. The effects of titanium and hydroxyapatite on osteoblastic expression and proliferation in rat parietal bone cultures. J Dent Res 1993;72:1005–1008.
23. McCulloch CA, Tenenbaum HC. Dexamethasone induces proliferation and terminal differentiation of osteogenic cells in tissue culture. Anat Rec 1986;215:397–402.
24. Jaiswal N, Haynesworth SE, Caplan AI, Bruder SP. Osteogenic differentiation of purified, culture-expanded human mesenchymal stem cells in vitro. J Cell Biochem 1997;64:295–312.
25. Shu R, McMullen R, Baumann MJ, McCabe LR. Hydroxyapatite accelerates differentiation and suppresses growth of MC3T3-E1 osteoblasts. J Biomed Mater Res A 2003;67:1196–1204.
26. Nishio K, Neo M, Akiyama H, Okada Y, Kokubo T, Nakamura T. Effects of apatite and wollastonite containing glass-ceramic powder and two types of alumina powder in composites on osteoblastic differentiation of bone marrow cells. J Biomed Mater Res 2001;55:164–176.
27. Loty C, Sautier JM, Tan MT, Oboeuf M, Jallot E, Boulekbache H, Greenspan D, Forest N. Bioactive glass stimulates in vitro osteoblast differentiation and creates a favorable template for bone tissue formation. J Bone Miner Res 2001;16:231–239.
28. Rhee S, Hwang M, Si HJ, Choi JY. Biological activities of osteoblast on poly (methyl methacrylate)/silica hybrid containing calcium salt. Biomaterials 2003;24:901–906.
29. Anderson SI, Downes S, Perry CC, Caballero AM. Evaluation of the osteoblast response to a silica gel in vitro. J Mater Sci Mater Med 1998;9:731–735.
30. Christodoulou I, Buttery LD, Saravanapavan P, Tai G, Hench LL, Polak JM. Dose- and time-dependent effect of bioactive gel-glass ionic-dissolution products on human fetal osteoblast-specific gene expression. J Biomed Mater Res B Appl Biomater 2005;74:529–537.
31. Ni S, Chang J, Chou L. A novel bioactive porous $CaSiO_3$ scaffold for bone tissue engineering. J Biomed Mater Res A 2006; 76:196–205.
32. Reffitt DM, Ogston N, Jugdaohsingh R, Cheung HF, Evans BA, Thompson RP, Powell JJ, Hampson GN. Orthosilicic acid stimulates collagen type1 synthesis and osteoblastic differentiation in human osteoblast-like cells in vitro. Bone 2003;32: 127–135.
33. Stein GS, Lian JB, Owen TA. Relationship of cell growth to the regulation of tissue-specific gene expression during osteoblast differentiation. FASEB J 1990;4:3111.
34. Mauney JR, Kirker-Head C, Abrahamson L, Gronowicz G, Volloch V, Kaplan DL. Matrix-mediated retention of in vitro osteogenic differentiation potential and in vivo bone-forming capacity by human adult bone marrow-derived mesenchymal stem cells during ex vivo expansion. J Biomed Mater Res A 2006;79:464–475.
35. Mauney JR, Kaplan DL, Volloch V. Matrix-mediated retention of osteogenic differentiation potential by human adult bone marrow stromal cells during ex vivo expansion. Biomaterials 2004;25:3233–3243.
36. Mauney JR, Volloch V, Kaplan DL. Matrix-mediated retention of adipogenic differentiation potential by human adult bone marrow-derived mesenchymal stem cells during ex vivo expansion. Biomaterials 2005;26:6167–6175.
37. Reinstorf A, Ruhnow M, Gelinsky M, Pompe W, Hempel U, Wenzel KW, Simon P. Phosphoserine-a convenient compound for modification of calcium phosphate bone cement collagen composites. J Mater Sci Mater Med 2004;15:451–455.